Available online at www.sciencedirect.com
ScienceDirect
Coordination Chemistry Reviews 251 (2007) 2665–2673
COORDINATION CHEMISTRY REVIEWS
www.elsevier.com/locate/ccr

Review

Control of magnetism by isomerization of intercalated molecules in organic–inorganic hybrid systems

N. Kojima [a,b,*], M. Okubo [c], H. Shimizu [a], M. Enomoto [a]

[a] *Department of Basic Science, Graduate School of Arts and Sciences, The University of Tokyo, Komaba 3-8-1, Meguro-ku, Tokyo 153-8902, Japan*
[b] *Institute for Molecular Science, Myodaiji, Okazaki 444-8787, Japan*
[c] *National Institute of Advanced Industrial Science and Technology, Umezono, 1-1-1 Tsukuba, Ibaraki 305-0012, Japan*

Received 31 December 2006; accepted 28 August 2007
Available online 1 September 2007

Contents

1. Introduction 2665
2. Experimental 2666
3. Organic–inorganic hybrid system, $Co_4(OH)_7(DAE)_{0.5}\cdot 3H_2O$ 2667
   3.1. Structure 2667
   3.2. Magnetic properties 2668
   3.3. Photomagnetism 2669
4. Organic–inorganic hybrid system $(DAE)CuCl_4$ 2670
   4.1. Structure 2670
   4.2. Magnetic properties 2670
   Acknowledgments 2672
   References 2672

Abstract

Intercalation of an organic photochromic molecule into layered magnetic systems has a possibility to provide multifunctional properties such as photomagnetism. In order to build up photosensitive multifunctional magnets, organic–inorganic hybrid systems coupled with photochromic diarylethene ion (DAE) and layered ferromagnets such as cobalt layered hydroxides (LDHs) and layered perovskite-type copper halides were synthesized. In the case of cobalt LDHs with DAE, $Co_4(OH)_7(DAE)_{0.5}\cdot 3H_2O$, the remarkable enhancement of the Curie temperature from 9 to 20 K was realized by substituting the open form of DAE with the closed form of DAE as intercalated molecule because of the delocalized π electrons in the closed form of DAE. By UV irradiation at 313 nm, $Co_4(OH)_7(DAE)_{0.5}\cdot 3H_2O$ shows the photoisomerization of DAE from the open form to the closed one in the solid state, which induces the enhancement of the Curie temperature. In the case of layered perovskite-type copper chlorides with a diarylethene cation $(DAE)CuCl_4$ with the open form of DAE, this shows the antiferromagnetic transition at $T_N = 3$ K, while $(DAE)CuCl_4$ with the closed form of DAE shows no magnetic phase transition above 2 K.

Keywords: Photochromic molecule; Molecular magnets; Ferromagnetism; Photoisomerization; Organic-inorganic hybrid system

1. Introduction

Current research in the field of molecular solids includes investigating the possibility of an organic–inorganic hybrid system having multifunctionality coupled with transport, optical or magnetic properties. Among these multifunctional materials based on molecular solids, extensive studies have been performed, both from the fundamental and applied points of

* Corresponding author at: Department of Basic Science, Graduate School of Arts and Sciences, The University of Tokyo, Komaba 3-8-1, Meguro-ku, Tokyo 153-8902, Japan. Tel.: +81 3 5454 6741; fax: +81 3 5454 6741.
E-mail address: cnori@mail.ecc.u-tokyo.ac.jp (N. Kojima).

0010-8545/$ – see front matter © 2007 Elsevier B.V. All rights reserved.
doi:10.1016/j.ccr.2007.08.025

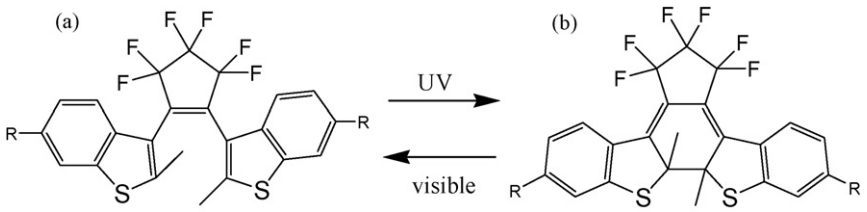

Scheme 1. 2,2′-Dimethyl-3,3′-(perfluorocyclopentene-1,2-diyl)bis(benzo[b]thiophene-6-R). (**1**: R = SO_3^-, **2**: R = NH_3^+). **1a**, **2a**: open form. **1b**, **2b**: closed form.

view, for various photo-induced phenomena such as the light-induced excited spin state trapping (LIESST) in spin-crossover complexes [1–3], the photo-induced magnetism in transition metal cyanides [4–8], the photo-induced valence transition for halogen-bridged gold mixed-valence complexes [9,10] and iodine-bridged binuclear Pt complexes [11], the photo-induced transition between the metallic and insulating phases for organic salts [12,13], and so forth.

Among various multifunctional materials, a molecular-based magnet is a leading candidate as a photo-controllable multifunctional material. Intercalated magnetic compounds such as layered hydroxides (LDHs) [14–18], oxalato-bridged bimetal compounds A[M(II)M′(III)$(ox)_3$] (A = cation, M, M′ = metal, $ox^{2-} = C_2O_4^{2-}$) [19–25], dithiooxalato-bridged bimetal compounds A[M(II)M′(III)$(dto)_3$] (A = cation, M, M′ = metal, $dto^{2-} = C_2S_2O_2^{2-}$) [26–32], or perovskite-type metal halides $A_2M(II)X_4$ (A = cation, M = metal, X = halogen) [33–35], provide an excellent opportunity to control their magnetic properties by the intercalation of various molecules. In particular, metal LDHs, $M_x(OH)_yA{\cdot}zH_2O$ (M = Cu, Co, A = organic anion), and perovskite-type metal halides, $A_2M(II)X_4$ (M = Cr, Cu), have tunable interlayer distances, which result in various types of magnetism such as ferromagnetism, ferrimagnetism or antiferromagnetism. Furthermore, in the case of metal LDHs, the number of double bonds in the bridging intercalated anion is an essential feature in controlling the type of magnetic interaction, that is, the ferromagnetic or antiferromagnetic interaction between layers [36,37].

In organic–inorganic hybrid systems, it is effective to use an organic photochromic molecule for producing photo-switchable materials. Based on this strategy, we have used photochromic diarylethene ions (**1**, **2**) as intercalated molecules for cobalt LDHs and layered perovskite-type copper chlorides. The open and closed forms of diarylethene (DAE) are converted into each other by UV and visible light irradiation, respectively. In general, DAE undergoes a thermally irreversible and fatigue-resistant photochromic reaction [38,39] (Scheme 1).

In this paper, we report the synthesis of organic–inorganic hybrid systems coupled with photochromic DAE ions and layered ferromagnets, $Co_4(OH)_7(\mathbf{1})_{0.5}{\cdot}3H_2O$ and $(\mathbf{2})CuCl_4$, and the control of their magnetic properties by means of the isomerization of intercalated photochromic DAE molecules [40–42].

2. Experimental

Reagents were of commercial grade. Perfluorocyclopentene was provided by NIHON ZEON. The sodium salt of the diarylethene anion, **1a**, was synthesized according to the literature [43–46]. The diarylethene cation salt, $(\mathbf{2a})Cl_2$, was also synthesized according to the literature [47–49]. $Co_2(OH)_3(CH_3COO){\cdot}H_2O$ was prepared as a blue colored powder through the precipitation method [18]. The sodium salt of the

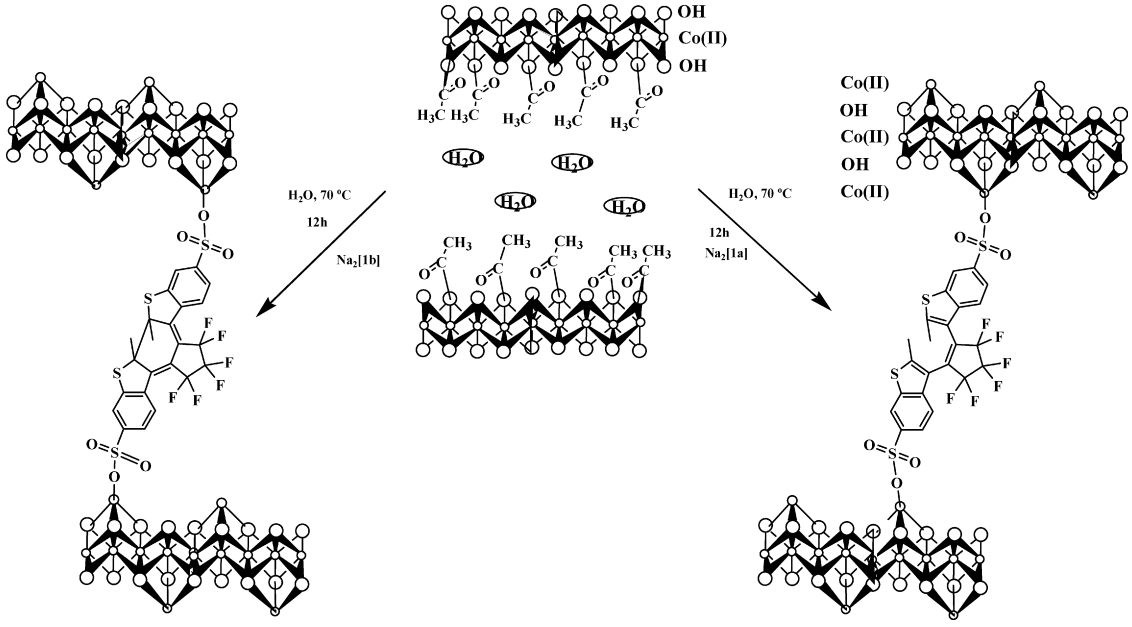

Scheme 2. Schematic representation of synthesis and crystal structures of co-LDHs intercalating open form (left) and closed form (right) of a DAE anion (**1**).

diarylethene anion, **1b**, was synthesized by applying UV light to the aqueous solution of **1a** with an Asahi Spectra LAX-101 xenon lamp for 2 h.

The intercalation compound, $Co_4(OH)_7$(**1a** or **1b**)$_{0.5}\cdot 3H_2O$ (=**3a** or **3b**), was prepared by an anion-exchange reaction between $Co_2(OH)_3(CH_3COO)\cdot H_2O$ and **1a** (or **1b**) as shown in Scheme 2.

The perovskite-type copper halide with the diarylethene cation, (**2a**)$CuCl_4$, was obtained as a yellowish green colored powder by mixing stoichiometric amounts of $CuCl_2$ and (**2a**)Cl_2 in methanol in the dark. The dark green compound (**2b**)$CuCl_4$ was also synthesized in a similar way, except the closed form of diarylethene cation salt, (**2b**)Cl_2, was used.

The dc and ac magnetic susceptibilities of powder samples were measured by Quantum Design MPMS5 SQUID susceptometer. The measuring temperature range for the dc susceptibility was between 2 and 300 K. The core diamagnetism, estimated by using Pascal's law, was subtracted from the total dc magnetic susceptibility. The ac susceptibility was measured in the temperature range between 2 and 40 K at a frequency of 375 Hz under an alternating field of 0.4 G. The ac magnetic susceptibility for the UV irradiated sample was measured after irradiating the powder sample of **3a**, spread on a glass slide, at 313 nm with light intensity of 40 mW/cm^2 for 1 day.

The *M–H* hysteresis curves were measured at 2 K in the magnetic field range from 5.0×10^4 to -5.0×10^4 G. For the measurement of *M–H* hysteresis curves, the powder sample was dispersed in liquid paraffin in order to block the motion of sample induced by an external magnetic field.

3. Organic–inorganic hybrid system, $Co_4(OH)_7(DAE)_{0.5}\cdot 3H_2O$

According to the recent molecular orbital calculation, the π electron system is divided at the contact between the benzothiophene and cyclopentene parts in the open form of DAE, while that of the closed form is connected from end to end of molecule by connection between two benzothiophene. Using this photoswitchable π electron system in DAE, the ends of which are modified by nitronylnitroxide radicals, as a photochromic spin coupler, Matsuda et al. succeeded in controlling the magnetic exchange interaction between two nitronyl nitroxide radicals by photoirradiation and they showed that the antiferromagnetic interaction between both sides of nitronyl nitroxide radicals is enhanced from $J/k_B = -2.2$ K in the open form to $J/k_B = -11.6$ K in the closed form [50,51]. By using a DAE anion as a magnetic coupler in order to change the magnetic properties of LDHs from a 2D to a 3D magnet, we have intercalated a DAE anion into Co-LDHs, in order to control the magnetism by photoisomerization of DAE.

3.1. Structure

As mentioned in the Section 2, the intercalation compound, $Co_4(OH)_7$(**1a** or **1b**)$_{0.5}\cdot 3H_2O$ (=**3a** or **3b**), was prepared by an anion-exchange reaction. The structural information in this research was obtained by powder X-ray diffraction. Fig. 1 shows the X-ray diffraction pattern of the parent compound, $Co_2(OH)_3(CH_3COO)\cdot H_2O$ (Fig. 1(a)) and the intercalation compound **3a** (Fig. 1(b)) [41]. As shown in Fig. 1, the strong (0 0 *l*) reflections of the parent compound disappear and new (0 0 *l*) reflections appear after the anion exchange reaction, which clearly indicates that the anion exchange reaction takes place successfully. Based on the (0 0 *l*) reflections corresponding to the interlayer distance, the interlayer distance of **3a** is estimated at 27.8 Å. Comparing with $Co_2(OH)_3(CH_3COO)\cdot H_2O$, the interlayer distance is expanded by 15 Å, which allows us to illustrate a schematic representation of Scheme 2. As shown in Scheme 2, the DAE anion, **1a**, is intercalated between the cobalt layers. From the analysis of the X-ray diffraction patterns of **3a** and **3b**, it was confirmed that both **1a** and **1b** are intercalated between the adjacent Co layers. The peaks of Co-LDHs intercalating the closed form of DAE are broader than those of Co-LDHs intercalating the open form of DAE since the open form of DAE coexists as a minor fraction with the closed form of DAE, which causes the disorder of **1b**. Estimated from Fig. 1, the interlayer distance of **3a** is 27.8 Å and that of **3b** is about 28 Å.

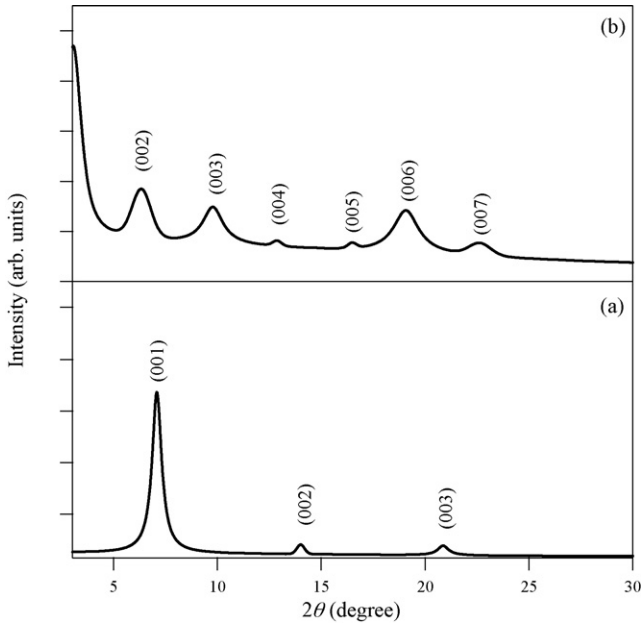

Fig. 1. Powder X-ray diffraction patterns for $Co_2(OH)_3(CH_3COO)\cdot H_2O$ (a) and **3a** (b) [41].

According to the literature [52], the crystal structure of Co-LDHs was reported to be characterized into two kinds of layer structures, *i.e.*, single-decker layer structure with only octahedral cobalt ions and triple-decker layer structure with both octahedral and tetrahedral cobalt ions. In general, a Co(II) ion tetrahedrally coordinated by four oxygen atoms is blue and a Co(II) ion octahedrally coordinated by six oxygen atoms is pale pink in color. Reflecting the color of octahedral and tetrahedral cobalt ions, Co-LDHs with single-decker layers and triple-decker layers display pale pink color and green color, respectively. Therefore, the green color of **3a** clearly indicates that the layers of **3a** contain the tetrahedral cobalt ions as well as the octahedral cobalt ions and is the triple-decker layer structure.

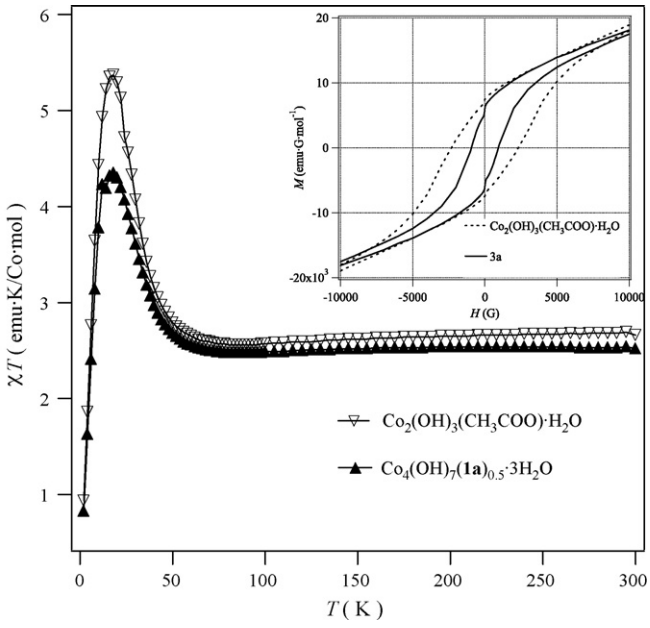

Fig. 2. χT as a function of temperature for $Co_2(OH)_3(CH_3COO)\cdot H_2O$ and **3a**. Inset shows the hysteresis loop of the magnetization for $Co_2(OH)_3(CH_3COO)\cdot H_2O$ (- - -) and **3a** (—) at 2 K.

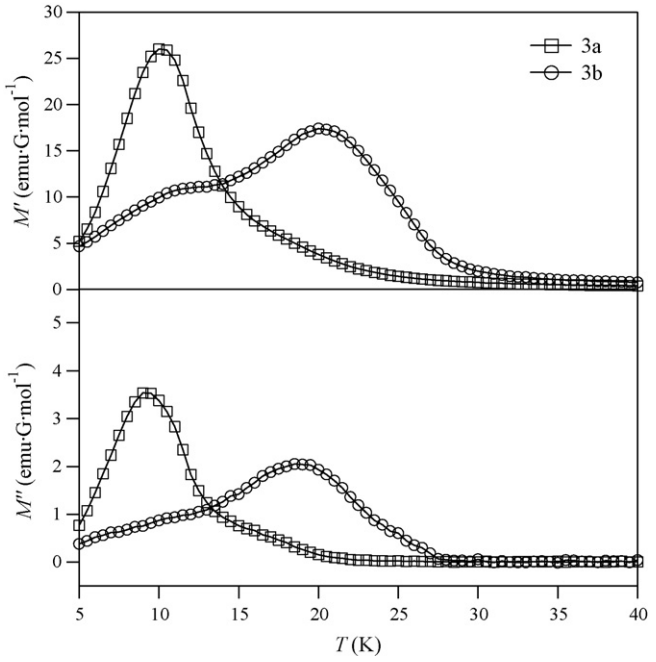

Fig. 3. Real (M') and imaginary (M'') part of ac magnetic susceptibility for **3a** (□) and **3b**(○) [42].

3.2. Magnetic properties

Fig. 2 shows the temperature dependence of χT and the M–H hysteresis curve for **3a** to clarify the intercalation effect on the magnetic properties of the cobalt LDHs. The temperature dependence of χT for $Co_2(OH)_3(CH_3COO)\cdot H_2O$ is also plotted for comparison. At room temperature, the χT value of **3a** is 2.52 emu K mol^{-1} per one cobalt, which is in agreement with the expected value (2.50 emu K mol^{-1}) for $S = 3/2$ with $g = 2.31$. The g value was obtained from EPR.

With decreasing temperature down to 60 K, the χT value of **3a** shows a slight decrease. This can be interpreted by two effects. First, an octahedrally coordinated Co(II) ion in a high spin state has an electron configuration of $t_{2g}^5 e_g^2$ ($S = 3/2$, $L = 1$). Therefore, the drop in μ_{eff} occurs due to the spin–orbit coupling as the temperature decreases, which can explain the decrease of the χT value of **3a**. Secondly, **3a** has a triple-decker structure as mentioned in the Section 3.1. In general, the tetrahedral Co(II) ion and octahedral Co(II) ion interact antiferromagnetically with each other [52]. Therefore, the decrease of the χT value can also be explained by the antiferromagnetic interaction between the tetrahedral and octahedral Co(II) ions. It is likely that both the drop in μ_{eff} of the octahedral Co(II) ion and the antiferromagnetic interaction between the octahedral Co(II) ion and the tetrahedral Co(II) ion contribute to the decrease of the χT value. Below 60 K, χT of **3a** increases sharply with a maximum around 20 K, which indicates a ferromagnetic or a ferrimagnetic transition at low temperature.

The temperature dependent ac magnetic susceptibilities of **3a** and **3b** are shown in Fig. 3. Judging from the temperature at the peak of magnetic susceptibility, the Curie temperatures are estimated at 9 and 20 K for **3a** and **3b**, respectively. The shoulder at 10 K for **3b** suggests a minor fraction with the open form of diarylethene.

Fig. 4 shows the interlayer distance dependence of the Curie temperature for various Co-LDHs [42]. In the case of Co-LDHs without π electron system in intercalated molecule, as the interlayer distance increases from 13 to 28 Å, the Curie temperature decreases from 14 to 8 K. In this case, the magnetic dipole–dipole interaction between the layers dominates

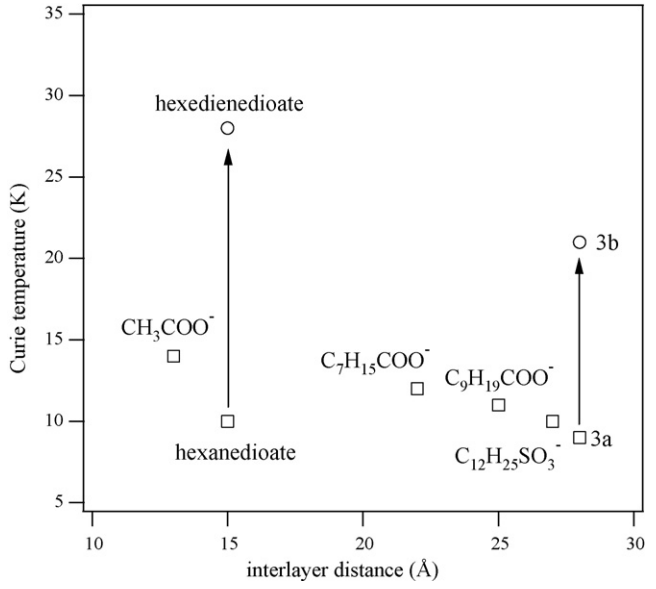

Fig. 4. The relation between the interlayer distance and the Curie temperature of Co-LDHs [42]. The Curie temperatures of Co-LDHs with CH_3COO^-, $C_7H_{15}COO^-$, $C_9H_{19}COO^-$ and $C_{12}H_{25}COO^-$ are quoted from ref. [15]. Arrows show the enhancement of Curie temperature induced by the π electron system of intercalated anions.

the variation of Curie temperature. In contrast, the Curie temperature (20 K) of **3b** is remarkably higher than that (9 K) of **3a**, although the interlayer distance of **3b** is almost as same as that of **3a**. Therefore, another stronger magnetic interaction should dominate the magnetic ordering in **3b**. As mentioned already, the closed form of DAE has the delocalized π electron system contrary to the open one of DAE in which the π electron system is divided at a contact between benzothiophene and cyclopentene parts.

Since the intralayer magnetic interaction is thought to be same in both **3a** and **3b**, the exchange coupling through the delocalized π electron system of the closed form of DAE should be responsible for the remarkable enhancement of the Curie temperature of **3b**. As shown in Fig. 4, similar remarkable enhancement of the Curie temperature was also observed in Co-LDHs with hexadienedioate having conjugated π electron system [42].

The importance of the π electron in the pillar molecule can also be proved theoretically. Since the Curie temperature of Co-LDHs without π electron system in intercalated molecule does not strongly depend on the interlayer distance as shown in Fig. 4, the magnetic dipole–dipole interaction is small enough to be ignored. Moreover, the ground high spin state of Co^{2+}, $^4T_1$, behaves as an Ising spin due to the strong spin–orbit interaction. The characteristic property of Ising spin is reflected in the large anisotropy of the g value in EPR, for example, Co^{2+} in TiO_2 has $g_x = 2.079$, $g_y = 5.885$, and $g_z = 3.735$ [53]. Thus, the magnetic interaction of Co-LDHs with various pillar molecules can be described as the Hamiltonian for a quasi two-dimensional Ising-type magnet with interaction between adjacent layers

$$H = -2J\sum\nolimits_{\text{intralayer}}(S_i^z S_j^z) - 2J\xi\sum\nolimits_{\text{interlayer}}(S_i^z S_j^z)$$

where ξ denotes a parameter of interlayer magnetic interaction taking its value from 0 to 1. The ξ dependence of the Curie temperature based on this Hamiltonian by employing Monte Carlo method [54] gives the ratio of the Curie temperature for the three-dimensional limit to the two-dimensional limit, $T_C(\xi = 1)/T_C(\xi = 0)$, as 2.0. This result strongly suggests the enhancement of the Curie temperature by introducing the interlayer exchange interaction through the delocalized π electron system. In fact, the ratio of the Curie temperatures for **3a** and **3b** is 2.2, which is close to the calculated ratio of the Curie temperature for the three-dimensional limit to the two-dimensional limit. Thus, **3a** can be described as a quasi two-dimensional magnetic system consisting of two-dimensional Ising type layers which interact with each other through the weak magnetic dipole–dipole interaction, while **3b** can be described as a quasi three-dimensional magnetic system consisting of two-dimensional Ising type layers which interact with each other through the strong exchange interaction via the delocalized π electron system of intercalated molecule. In the case of **3a**, the intralayer exchange interaction is estimated at $J_{\text{intra}}/k_B = 6.7$ K, according to the theory of the 2D Ising model [55].

3.3. Photomagnetism

The drastic change between quasi two-dimensional magnetic system of **3a** and quasi three-dimensional magnetic system of **3b** suggests the possibility to control the magnetic transition in the solid state by photo-isomerization of DAE.

The absorption spectra of **3a** in a KBr pellet were measured as a function of light irradiation at room temperature to probe the photochromism of **1a** in **3a** [41]. In order to exclude the absorption of the inorganic layer for clarity, absorption spectroscopic changes from the initial state upon light irradiation at 313 and 550 nm are shown in Fig. 5(a) and (b), respectively. With light irradiation at 313 nm, broad absorption bands around 400 and 550 nm appear, which correspond to the π–π* transitions for the photocyclized isomer, **1b** (Fig. 5(a)). After 15 min, it reaches the photo-stationary state, where the color of the pellet changes from green to red-purple. When the pellet is irradiated with light of 550 nm, the absorption bands around 400 and 550 nm decrease (Fig. 5(b)) and the color of the pellet returns to green after 30 min, which suggests that **1b** is returned to **1a** by light irradiation at 550 nm. In other words, reversible photochromism of **1a** occurs in the solid state.

Fig. 6 shows the ac magnetic susceptibilities as a function of temperature for **3a** before and after UV irradiation at 313 nm at room temperature [42]. As shown in Fig. 6, after UV irradiation at 313 nm, the shoulder of ac magnetic susceptibility emerged at about 18 K. From the similarity between the temperature of this shoulder and the temperature at the peak top of ac magnetic susceptibility for **3b**, this shoulder implies the appearance of the ferromagnetic phase with the closed form of DAE (**1b**) in **3a**. Since the photoisomerization partially occurs on the surface of the compound, the magnitude of the shoulder is small compared with the peak of the ac magnetic susceptibility for **3b**. In the

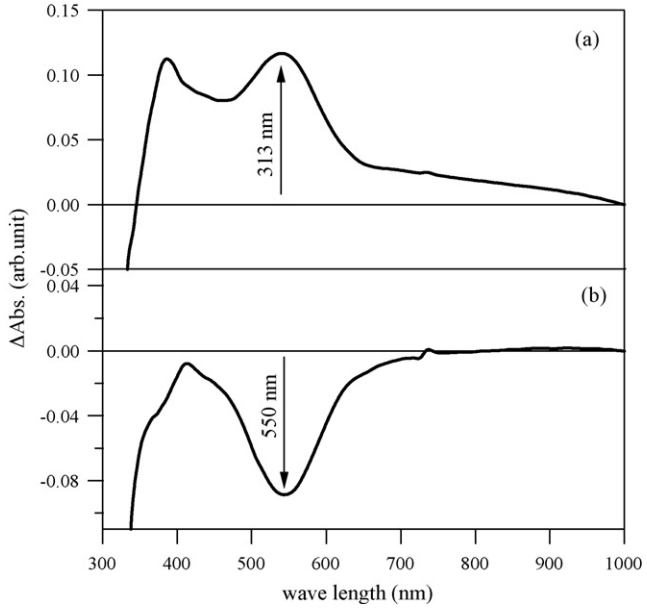

Fig. 5. UV–vis absorption spectroscopic changes of **3a** from the initial state upon (a) 313 nm irradiation and (b) 550 nm irradiation, where ΔAbs. = absorbance (after irradiation) − absorbance (before irradiation) at 300 K [41].

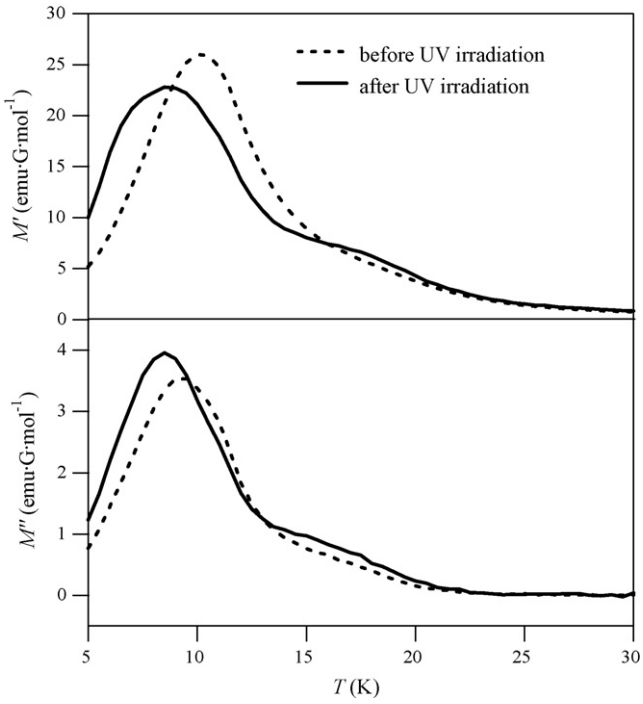

Fig. 6. Real (M') and imaginary (M'') part of ac magnetic susceptibility of **3a** before UV irradiation (- - -) and after UV irradiation (—) [42].

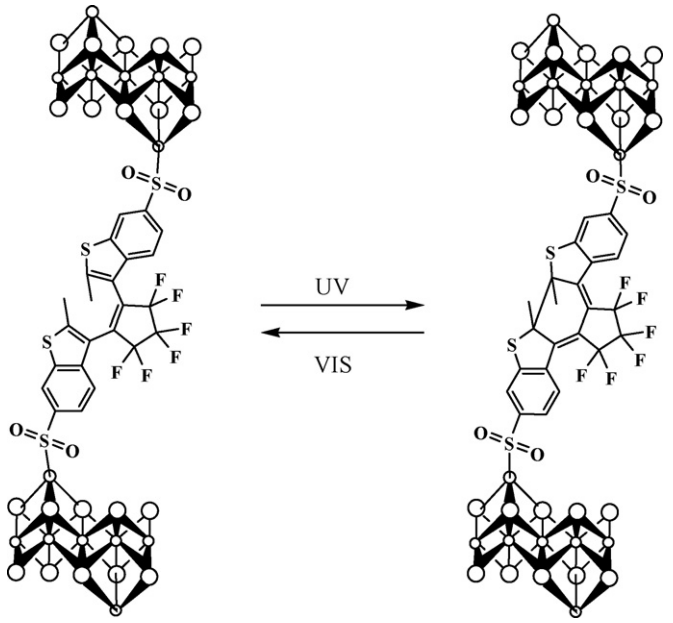

Scheme 3. Schematic representation of the photo-induced conversion between Co-LDHs with the open-form of DAE (left) and Co-LDHs with closed-form of DAE (right).

case of **3a**, UV irradiation at 313 nm does not completely penetrate into the sample because of the strong optical absorption corresponding to the π–π* transition of DAE.

Therefore, the UV irradiated **3a** should have two domains corresponding to **3a** and **3b**. The conversion ratio of DAE from the open form to the closed one in **3a** is estimated to be less than 5 % based on the AC magnetic susceptibility. In order to avoid the π–π* absorption of DAE and produce a prominent photoconversion from **3a** to **3b** (Scheme 3), the photoisomerization of DAE induced by two-photon excitation with 630 nm light is indispensable and in progress.

As described in Scheme 3, this character gives us the possibility for photo-switchable paramagnetic–ferromagnetic transformations in the temperature region between 9 and 20 K because UV irradiation provides the ferromagnetic phase of **3b**, while visible light provides the paramagnetic phase of **3a** in this temperature region. When the photoisomerization occurs in this temperature region, we can select the magnetism as the paramagnetic phase with **3a** or the ferromagnetic phase with **3b** by selecting the wavelength of irradiated light.

4. Organic–inorganic hybrid system (DAE)$CuCl_4$

Layered perovskite-type copper halides with intercalated organic molecules have the general formula $[R(NH_3)]_2CuCl_4$ (R = organic molecule). They consist of layers of corner-sharing $CuCl_6$ octahedra sandwiched by the organic cations. Their magnetic properties have been well studied and they are known as two-dimensional ferromagnets governed by the cooperative Jahn–Teller effect [33]. There is a simple relation between the Jahn–Teller prolonged Cu–Cl bond distance d and the magnitude of the intralayer interaction J [34]. If the photoisomerization of an intercalated photochromic molecule occurs efficiently in these layered perovskite-type copper halides, then d and J can be expected to be reversibly controlled. According to ref. [56], the cooperative Jahn–Teller effect of the $CuCl_4$ layer in $[R(NH_3)]_2CuCl_4$ provides considerable flexibility, which makes it possible to intercalate bulky cations into the lattice. In this section, we report the magnetic properties of an organic–inorganic hybrid system (DAE)$CuCl_4$ (Scheme 4).

4.1. Structure

A single crystal X-ray structural analysis was carried out for (**2a**)$CuCl_4$. The atomic coordinates of the intercalated organic layer could not be determined since the closed form of DAE coexists as a minor fraction with the open form of DAE, which causes the disorder of **2a**, but the atomic coordinates of the inorganic $CuCl_4$ layer could be determined. The crystallographic data for (**2a**)$CuCl_4$ are as follows: triclinic, $P1$, $a = 7.914(16)$ Å, $b = 14.138$ Å, $c = 24.638(49)$ Å, $\alpha = 100.21(4)^\circ$, $\beta = 99.28(4)^\circ$, $\gamma = 90.06(5)^\circ$, $V = 2676.2$ Å^3, $Z = 4$. Powder X-ray diffraction measurements were carried out to clarify the difference between the crystal structures of (**2a**)$CuCl_4$ and (**2b**)$CuCl_4$. The interlayer distance of (**2b**)$CuCl_4$ is slightly shorter (∼0.6 Å) than that (24.638(49) Å) of (**2a**)$CuCl_4$, which is due to the isomerization of DAE. Scheme 4 shows the schematic structure of (**2a**)$CuCl_4$.

4.2. Magnetic properties

Fig. 7 shows the magnetic susceptibilities as a function of temperature for (**2a**)$CuCl_4$ and (**2b**)$CuCl_4$ [40]. Both the χ values increase with decreasing temperature. The inset shows χT as a function of temperature for both compounds. The χT val-

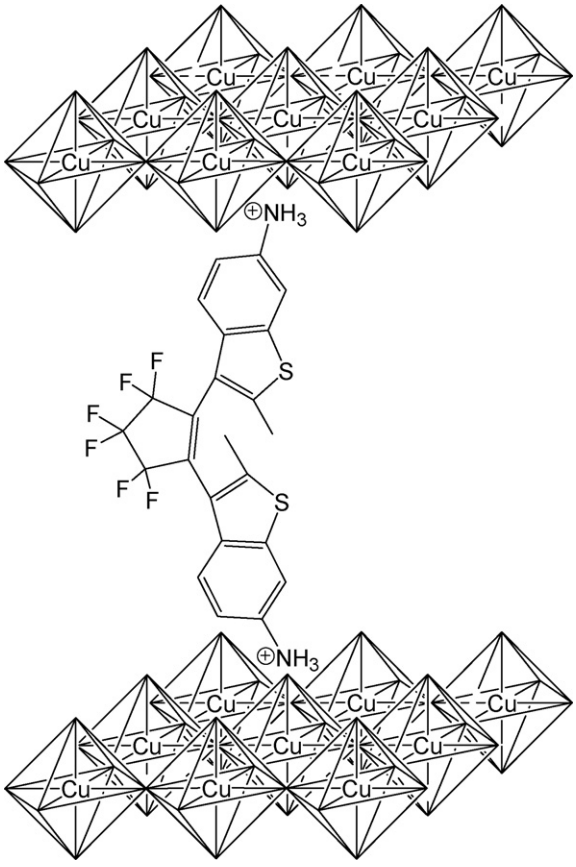

Scheme 4. Schematic structure of (**2a**)$CuCl_4$.

ues also increase with decreasing temperature, which clearly indicates a ferromagnetic intralayer interaction.

The solid lines in Fig. 7 denote the fitted magnetic susceptibility by means of the high-temperature series expansion for a two-dimensional Heisenberg ferromagnet on a quadratic lattice [57,58]:

$$\frac{\chi T}{C} = 1 + 2\left(\frac{J}{k_B T}\right) + 2\left(\frac{J}{k_B T}\right)^2 + \frac{3}{4}\left(\frac{J}{k_B T}\right)^3 + \frac{13}{12}\left(\frac{J}{k_B T}\right)^4 + \cdots$$

where C is the Curie constant for $S = 1/2$ and $g = 2.11$ and k_B is the Boltzmann constant. The g value was obtained from EPR. The least-square fitting gives the value of J/k_B for (**2a**)$CuCl_4$ and (**2b**)$CuCl_4$ as 10.7 and 6.9 K, respectively.

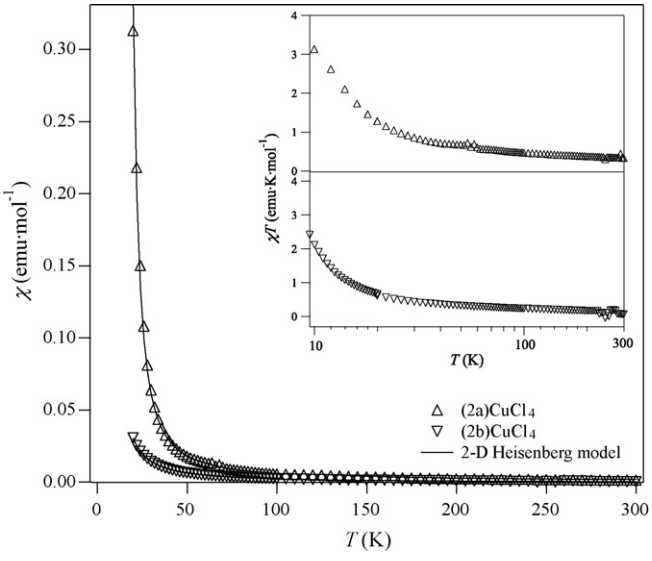

Fig. 7. Temperature dependence of the magnetic susceptibilities of (**2a**)$CuCl_4$ and (**2b**)$CuCl_4$. The solid curves denote the calculated susceptibility by means of the high-temperature series expansion for a two-dimensional Heisenberg ferromagnet on a quadratic lattice [40]. Inset shows χT as a function of temperature for (**2a**)$CuCl_4$ and (**2b**)$CuCl_4$.

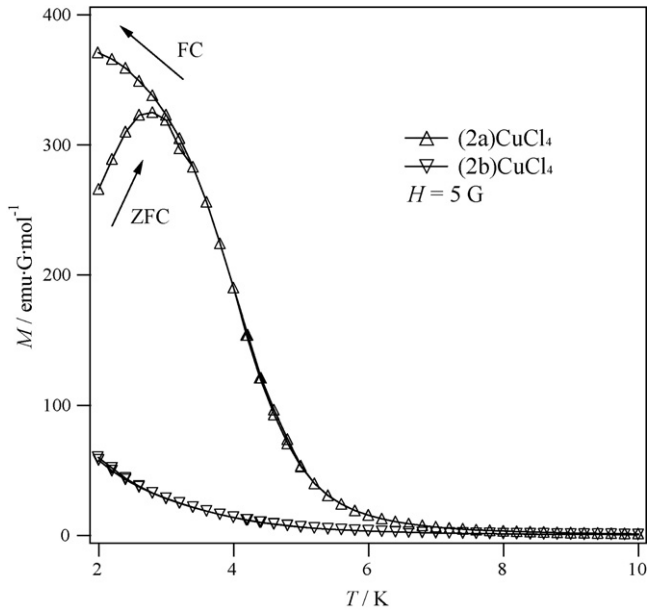

Fig. 8. Temperature dependence of the magnetizations of (**2a**)$CuCl_4$ and (**2b**)$CuCl_4$; ZFC and FC means the zero field cooled magnetization and the field cooled magnetization, respectively [40].

Below 10 K, the difference between the magnetizations of two salts appears to be obvious. As shown in Fig. 8, the field cooled magnetization of (**2a**)$CuCl_4$ shows a rapid increase below 6 K and almost saturates at 3 K. The zero field cooled magnetization and field cooled magnetization curves meet at about 3 K, where a magnetic phase transition takes place. In fact, both the real and imaginary parts of ac magnetic susceptibility for (**2a**)$CuCl_4$ show a maximum at 3.4 K, which clearly indicates a magnetic phase transition. Since the *M–H* curve at 2 K shows a meta-magnetism around 10 G, the magnetic phase transition is regarded as the antiferromagnetic transition with $T_N = 3.4$ K, which implies the antiferromagnetic interlayer interaction in (**2a**)$CuCl_4$. (**2b**)$CuCl_4$ shows no magnetic transition above 2 K in spite of the fact that the closed form of DAE, **2b**, has the delocalized π electron system and the interlayer distance of (**2b**)$CuCl_4$ is shorter (∼0.6 Å) than that of (**2a**)$CuCl_4$. As mentioned in the Section 3, the closed form of DAE with delocalized π electron system enhances the interlayer exchange coupling for **3b**. Therefore, the disappearance of the magnetic transition above 2 K in (**2b**)$CuCl_4$ is attributed not to a weaker interlayer magnetic

interaction but to a weaker intralayer magnetic interaction than that in (**2a**)$CuCl_4$. In connection with this, the relationship between the coordination geometry of the $CuCl_4$ layer and the intralayer magnetic interaction should be mentioned. In the case of (**2a**)$CuCl_4$, the most distorted Cu–Cl–Cu angle is 156°, which is far from the orthogonal arrangement of the magnetic orbital needed for the ferromagnetic interaction. Although the atomic coordinates of the $CuCl_4$ layer in (**2b**)$CuCl_4$ has not been determined, the larger distortion in the $CuCl_4$ layer due to the photo-cyclized isomer, **2b**, presumably take place in (**2b**)$CuCl_4$, which causes a weaker intralayer interaction for (**2b**)$CuCl_4$ than that for (**2a**)$CuCl_4$.

As previously mentioned in ref. [56], the cooperative Jahn–Teller effect of $[R(NH_3)_2]CuCl_4$ salts has been shown to provide considerable flexibility, which makes it possible to intercalate bulky cations into the lattice. In fact, the bulky cations, **2a** and **2b**, could be intercalated into the $CuCl_4$ layers due to this flexibility. The Mn or Cd salts, which are free from the Jahn–Teller effect, do not have this flexibility [59,60]. In fact, (**2a**)$MnCl_4$ is paramagnetic and therefore the $MnCl_4^{2-}$ anions should not form corner-sharing $MnCl_6$ octahedra layers, but be isolated in (**2a**)$MnCl_4$.

Acknowledgments

The authors wish to thank Prof. M. Irie for his kind advice on the synthesis of diarylethene. The authors are grateful to NIHON ZEON for the supply of perfluorocyclopentene. This work was supported by a Grant-in-aid for Scientific Research and a Grant-in-aid of 21st century COE (Center of Excellence) Program from the Ministry of Education, Culture, Sports, Science and Technology, Japan. One of the authors (M. Okubo) was supported by Research Fellowships of the Japan Society for the Promotion of Science for Young Scientists.

References

[1] S. Decurtins, P. Gütlich, C.P. Köhler, H. Spiering, A. Hauser, Chem. Phys. Lett. 105 (1984) 1.
[2] S. Decurtins, P. Gütlich, K.M. Hasselbach, A. Hauser, H. Spiering, Inorg. Chem. 24 (1985) 2174.
[3] P. Gütlich, H.A. Goodwin (Eds.), Spin Crossover in Transition Metal Compounds I–III, Springer, 2004, and references therein.
[4] O. Sato, T. Iyoda, A. Fujishima, K. Hashimito, Science 272 (1996) 704.
[5] Y. Einaga, O. Sato, T. Iyoda, Y. Kobashi, F. Ambe, K. Hashimoto, A. Fujishima, Chem. Lett. (1997) 289.
[6] F. Varret, A. Bleuzen, K. Boukheddaden, A. Bousseksou, E. Codjovi, C. Enachescu, A. Goujon, J. Linares, N. Menendez, M. Verdaguer, Pure Appl. Chem. 74 (2002) 2159.
[7] A. Bleuzen, C. Lomenech, V. Escax, F. Villain, F. Varret, C. Moulin, M. Verdaguer, J. Am. Chem. Soc. 122 (2000) 6648.
[8] A. Dei, Angew. Chem. Int. Ed. 44 (2005) 1160.
[9] J.-Y. So, T. Mizokawa, J.W. Quilty, K. Takubo, K. Ikeda, N. Kojima, Phys. Rev. B 72 (2005) 235105.
[10] X.J. Liu, Y. Moritomo, A. Nakamura, N. Kojima, J. Phys. Soc. Jpn. 68 (1999) 3134.
[11] H. Matsuzaki, T. Matsuoka, H. Kishida, K. Takizawa, H. Miyasaka, K. Sugiura, M. Yamashita, H. Okamoto, Phys. Rev. Lett. 90 (2003) 046401.
[12] M. Chollet, L. Guerin, N. Uchida, S. Fukaya, H. Shimoda, T. Ishikawa, K. Matsuda, T. Hasegawa, A. Ohta, H. Yamochi, G. Saito, R. Tazaki, S. Adachi, S. Koshihara, Science 307 (2005) 86.
[13] N. Uchida, S. Koshihara, T. Ishikawa, A. Ota, S. Fukaya, C. Matthieu, H. Yamochi, G. Saito, J. Phys. IV France 114 (2004) 143.
[14] P. Rabu, Z.L. Huang, C. Hornick, M. Drillon, Synth. Metals 122 (2001) 509.
[15] V. Laget, C. Hornick, P. Rabu, M. Drillon, R. Ziessel, Coord. Chem. Rev. 178 (1998) 1533.
[16] V. Laget, C. Hornick, P. Rabu, J. Mater. Chem. 9 (1999) 169.
[17] W. Fujita, K. Awaga, J. Am. Chem. Soc. 119 (1997) 4563.
[18] W. Fujita, K. Awaga, Inorg. Chem. 35 (1996) 1915.
[19] H. Tamaki, Z.J. Zhong, N. Matsumoto, S. Kida, M. Koikawa, N. Achiwa, Y. Hashimoto, H. Ōkawa, J. Am. Chem. Soc. 114 (1992) 6974.
[20] H. Tamaki, M. Mitsumi, K. Nakamura, N. Matsumoto, S. Kida, H. Ōkawa, S. Iijima, Chem. Lett. (1992) 1975.
[21] S. Decurtins, H.W. Schmalle, H.R. Oswald, A. Linden, J. Ensling, P. Gütlich, A. Hauser, Inorg. Chim. Acta 216 (1994) 65.
[22] R. Clement, S. Decurtins, M. Gruselle, C. Train, Monatsh. Chem. 134 (2003) 117.
[23] C. Mathonière, C.J. Nuttall, S.G. Carling, P. Day, Inorg. Chem. 35 (1996) 1201.
[24] E. Coronado, J.R. Galán-Mascarós, C.J. Gómez-García, J. Ensling, P. Gütlich, Chem. Eur. J. 6 (2000) 552.
[25] E. Coronado, J.R. Galán-Mascarós, C.J. Gómez-García, V. Laukhin, Nature 408 (2000) 447.
[26] H. Ōkawa, M. Mitsumi, M. Ohba, M. Kodera, N. Matsumoto, Bull. Chem. Soc. Jpn. 67 (1994) 2139.
[27] N. Kojima, W. Aoki, M. Itoi, M. Seto, Y. Kobayashi, Yu. Maeda, Solid State Commun. 120 (2001) 165.
[28] T. Nakamoto, Y. Miyazaki, M. Itoi, Y. Ono, N. Kojima, M. Sorai, Angew. Chem. Int. Ed. 40 (2001) 4716.
[29] Y. Kobayashi, M. Itoi, N. Kojima, K. Asai, J. Phys. Soc. Jpn. 71 (2002) 3016.
[30] Y. Ono, M. Okubo, N. Kojima, Solid State Commun. 126 (2003) 291.
[31] M. Itoi, A. Taira, M. Enomoto, N. Matsushita, N. Kojima, Y. Kobayashi, K. Asai, K. Koyama, T. Nakamoto, Y. Uwatoko, J. Yamaura, Solid State Commun. 130 (2004) 415.
[32] M. Itoi, Y. Ono, N. Kojima, K. Kato, K. Osaka, M. Takata, Eur. J. Inorg. Chem. (2006) 1198.
[33] L.J. de Jongh, W.D. van Amstel, A.R. Miedema, Physica 58 (1972) 277.
[34] C.P. Landee, K.E. Halvorson, R.D. Willett, J. Appl. Phys. 61 (1987) 3295.
[35] L.J. de Jongh (Ed.), Magnetic Properties of Layered Transition Metal Compounds, Kluwer Academic Publishers, Dordrecht, 1990.
[36] C. Hornick, P. Rabu, M. Drillon, Polyhedron 19 (2000) 259.
[37] P. Rabu, M. Drillon, K. Awaga, W. Fujita, T. Sekine, in: J.S. Miller, M. Drillon (Eds.), Magnetism: Molecules to Materials II, WILEY-VCH, 2001, p. 357.
[38] J.C. Crano, R.J. Gugliemetti (Eds.), Organic Photochromic and Thermochromic Compounds, vol. 1, Plenum Press, 1999 (Chapter 5).
[39] M. Irie, Chem. Rev. 100 (2000) 1685.
[40] M. Okubo, M. Enomoto, N. Kojima, Synth. Metals 152 (2005) 461.
[41] M. Okubo, M. Enomoto, N. Kojima, Solid State Commun. 134 (2005) 777.
[42] H. Shimizu, A. Nakamoto, M. Enomoto, N. Kojima, Inorg. Chem. 45 (2006) 10240.
[43] D.A. Shirley, M.D. Cameron, J. Chem. Soc. 74 (1952) 664.
[44] D.A. Shirley, M.J. Danzig, F.C. Canter, J. Am. Chem. Soc. 75 (1953) 3278.
[45] M. Hanazawa, R. Sumiya, Y. Horikawa, M. Irie, J. Chem. Soc. Chem. Commun. (1992) 206.
[46] M. Takeshita, N. Kato, S. Kawauchi, T. Imase, J. Watanabe, M. Irie, J. Org. Chem. 63 (1998) 9306.
[47] S. Kobatake, M. Yamada, T. Yamada, M. Irie, J. Am. Chem. Soc. 121 (1999) 8450.
[48] M. Yamada, M. Takeshita, M. Irie, Mol. Cryst. Liq. Cryst. 345 (2000) 107.
[49] M. Takeshita, M. Yamada, N. Kato, M. Irie, J. Chem. Soc. Perkin Trans. 2 (2000) 619.
[50] K. Matsuda, M. Irie, J. Am. Chem. Soc. 122 (2000) 7195.
[51] K. Matsuda, M. Irie, Chem. Eur. J. 7 (2001) 3466.
[52] M. Kurmoo, in: P. Day, A.E. Underhill (Eds.), Metal-Organic and Organic Molecular Magnets, The Royal Society, 1999, p. 185.

[53] P.P. Charles Jr., A.F. Horacio (Eds.), Handbook of Electron Spin Resonance, vol. 2, Springer-Verlag, 1999.
[54] S. Todo, S. Miyashita, private communication.
[55] M. Drillon, C. Hornick, V. Laget, P. Rabu, F.M. Romero, S. Rouba, G. Ulrich, R. Ziessel, Mol. Cryst. Liq. Cryst. 273 (1995) 125.
[56] R.D. Willett, H. Place, M. Middleton, J. Am. Chem. Soc. 110 (1988) 8639.
[57] G.A. Baker, H.E. Gilbert, J. Eve, G.S. Rushbrooke, Phys. Lett. A 25 (1967) 207.
[58] L.J. de Jongh (Ed.), Magnetic Properties of Layered Transition Metal Compounds, Kluwer Academic Publishers, 1990.
[59] L.O. Snively, P.L. Seifert, K. Emerson, J.E. Drumheller, Phys. Rev. B 20 (1979) 2101.
[60] B. Morosin, P. Fallon, J.S. Valentine, Acta Cryst. B 31 (1975) 2220.